

C-X-C Motif Chemokine Receptor 4 Blockade Promotes Tissue Repair After Myocardial Infarction by Enhancing Regulatory T Cell Mobilization and Immune-Regulatory Function

Running Title: *Wang et al.; CXCR4 Blockade Augments Regulatory T Cell Function*

Yong Wang, MD^{1,2}; Klaus Dembowski, MD, PhD³; Eric Chevalier, PhD³; Philipp Stüve, MS⁴; Mortimer Korf-Klingebiel, PhD^{1,2}; Matthias Lochner, PhD⁴; L. Christian Napp, MD²; Heike Frank, MD^{1,2}; Eva Brinkmann, BS^{1,2}; Anna Kanwischer, BS^{1,2}; Johann Bauersachs, MD²; Mariann Gyöngyösi, MD, PhD⁵; Tim Sparwasser, MD⁴; Kai C. Wollert, MD^{1,2}

¹Division of Molecular and Translational Cardiology, Department of Cardiology and Angiology, Hannover Medical School, Hannover, Germany; ²Department of Cardiology and Angiology, Hannover Medical School, Hannover, Germany; ³Polyphor Ltd., Allschwil, Switzerland; ⁴Institute of Infection Immunology, TWINCORE, Hannover, Germany; ⁵Division of Cardiology, Department of Internal Medicine II, Medical University of Vienna, Vienna, Austria

Address for Correspondence:

Kai C Wollert, MD
Department of Cardiology and Angiology
Hannover Medical School, Carl-Neuberg-Straße 1
30625 Hannover, Germany
Tel: +49-511-532-4055
Fax: +49-511-532-5307
Email: wollert.kai@mh-hannover.de

Abstract

Background: Acute myocardial infarction (MI) elicits an inflammatory response that drives tissue repair and adverse cardiac remodeling. Inflammatory cell trafficking after MI is controlled by C-X-C motif chemokine ligand 12 (CXCL12) and its receptor, C-X-C motif chemokine receptor 4 (CXCR4). CXCR4 antagonists mobilize inflammatory cells and promote infarct repair, but the cellular mechanisms are unclear.

Methods: We investigated the therapeutic potential and mode of action of the peptidic macrocycle CXCR4 antagonist POL5551 in mice with reperfused MI. We applied cell depletion and adoptive transfer strategies using lymphocyte-deficient *Rag1* knockout mice; DERE mice, which express a diphtheria toxin receptor-enhanced green fluorescent protein fusion protein under the control of the promoter/enhancer region of the regulatory T (T_{reg}) cell-restricted Foxp3 transcription factor; and dendritic cell-depleted CD11c-Cre iDTR mice. Translational potential was explored in a porcine model of reperfused MI employing serial contrast-enhanced MRI.

Results: Intraperitoneal POL5551 injections in wild-type mice (8 mg/kg at 2, 4, 6, and 8 d) enhanced angiogenesis in the infarct border-zone, reduced scar size, and attenuated left ventricular remodeling and contractile dysfunction at 28 d. Treatment effects were absent in splenectomized wild-type mice, *Rag1* knockout mice, and T_{reg} cell-depleted DERE mice. Conversely, treatment effects could be transferred into infarcted splenectomized wild-type mice by transplanting splenic T_{reg} cells from POL5551-treated infarcted DERE mice. Instructive cues provided by infarct-primed dendritic cells were required for POL5551's treatment effects. POL5551 injections mobilized T_{reg} cells into the peripheral blood followed by enhanced T_{reg} cell accumulation in the infarcted region. Neutrophils, monocytes, and lymphocytes displayed similar mobilization kinetics, but their cardiac recruitment was not affected. POL5551, however, attenuated inflammatory gene expression in monocytes and macrophages in the infarcted region via T_{reg} cells. Intravenous infusion of the clinical-stage POL5551 analogue POL6326 (3 mg/kg at 4, 6, 8, and 10 d) decreased infarct volume and improved left ventricular ejection fraction in pigs. **Conclusions:** Our data confirm CXCR4 blockade as a promising treatment strategy after MI. We identify dendritic cell-primed splenic T_{reg} cells as the central arbiters of these therapeutic effects and thereby delineate a pharmacological strategy to promote infarct repair by augmenting T_{reg} cell function *in vivo*.

Key Words: acute myocardial infarction; regulatory T cells; dendritic cells; C-X-C motif chemokine receptor 4; tissue repair; inflammation

Clinical Perspective

What is new?

- Inflammatory cell trafficking between hematopoietic organs and sites of tissue injury is controlled by CXCL12 and its receptor CXCR4. We show that bolus injections of a highly selective peptidic macrocycle CXCR4 antagonist enhance tissue repair and functional recovery after reperfused acute myocardial infarction in mice.
- The therapeutic effects require dendritic cell priming and are specifically mediated by T_{reg} cells. Intermittent CXCR4 blockade mobilizes T_{reg} cells from their splenic reservoir, leading to their enhanced recruitment to the infarcted region and T_{reg} cell-dependent attenuation of inflammatory gene expression in monocytes and macrophages.
- Highlighting the translational potential of this strategy, CXCR4 blockade also reduces infarct volume and improves systolic function in a porcine closed-chest model of reperfused acute myocardial infarction.

What are the clinical implications?

- This study outlines a new pharmacological approach to augment T_{reg} cell function and tissue repair after acute myocardial infarction.
- These findings should stimulate further research into the therapeutic potential of CXCR4 blockade after myocardial infarction and in other acute conditions wherein excessive innate and/or adaptive immune responses cause immunopathology.

Introduction

Acute myocardial infarction (MI) is caused by thrombotic occlusion of a coronary artery, leading to progressive cell death in the nonperfused territory. Improved reperfusion strategies have enhanced myocardial salvage in most patients with acute MI,¹ but patients with extensive myocardial injury remain at risk of developing chronic heart failure.² MI triggers an inflammatory response that leads to the necrotic area being replaced with highly vascularized granulation tissue and eventually a collagen-rich scar. The heart can undergo deleterious changes in left ventricular (LV) geometry and function during this vulnerable period before scar formation has stabilized the infarct area. The inflammatory response must therefore be tightly regulated to promote healing and prevent postinfarction heart failure.^{3,4}



Inflammatory cell trafficking from hematopoietic organs to sites of tissue injury is coordinated by chemokine-chemokine receptor networks.⁵ Several chemokines produced in the infarcted myocardium provide exit cues for circulating leukocytes expressing their cognate receptors.⁶⁻⁸ Therapeutically modulating chemokine-chemokine receptor interactions may promote infarct healing by limiting excessive inflammation-induced tissue damage or by enhancing the recruitment of angiogenic cell populations to the infarct wound.⁹⁻¹¹ Pharmacological blockade of the C-X-C motif chemokine receptor 4 (CXCR4) with the small molecule antagonists plerixafor (AMD3100) and burixafor (TG-0054) has been shown to improve heart function after MI in mice and pigs, respectively.¹⁰⁻¹² Plerixafor is clinically used to mobilize CXCR4-expressing hematopoietic stem and progenitor cells (HSPCs) from the bone marrow to the peripheral blood for collection and subsequent transplantation in patients with hematological malignancies.¹³ Under steady state conditions, HSPCs are retained in the bone marrow by interacting with the CXCR4 ligand, C-X-C motif chemokine ligand 12 (CXCL12),

which is constitutively produced by bone marrow stromal cells.¹⁴ After MI, CXCL12 expression increases in the infarct area and serves as a homing signal for circulating stem and progenitor cells and proangiogenic cell populations referred to as endothelial progenitor cells (EPCs).¹⁵⁻¹⁸ Along these lines, the beneficial effects of plerixafor after MI have been associated with enhanced mobilization and cardiac recruitment of EPCs and increased infarct vascularization.^{10,11} CXCR4, however, is widely expressed in the hematopoietic system,¹⁹ and HSPC mobilization by CXCR4 antagonists is accompanied by marked leukocytosis affecting all hematopoietic lineages in patients and mice.²⁰ Notably, neither HSPCs, EPCs, nor any specific myeloid or lymphoid cell population have been causally linked to the beneficial effects of CXCR4 blockade after MI.

POL5551 and its close analogue and clinical-stage compound POL6326 are potent, selective, and reversible CXCR4 antagonists that have been developed by protein epitope mimetics technology.²¹⁻²³ Both compounds are peptidic macrocycles that mimic the β -hairpin structure of the CXCR4-binding motif of CXCL12. Here, we investigated the therapeutic potential and mode of action of POL5551 in a mouse model of reperfused acute MI. We show that POL5551 promotes tissue repair and functional adaptation after MI via Foxp3⁺ regulatory T (T_{reg}) cells. Supporting the translational potential of this strategy, we find that POL6326 enhances systolic function in a porcine closed-chest model of reperfused acute MI. Our observations define a specific mode of action of CXCR4 blockade after MI and outline a new pharmacological approach to enhance T_{reg} cell function and tissue repair after acute MI.

Methods

Upon reasonable request, the data, analytic methods, and study materials will be made available to other researchers for the purposes of reproducing the results. Extended methods are provided

in the Supplemental Methods section in the Data Supplement.

Reagents

The CXCR4 antagonists POL5551 and POL6326 were provided by Polyphor.^{21,22} Mice were treated with POL5551 (8 mg/kg per dose) or POL6326 (8 mg/kg per dose), pigs with POL6326 (3 mg/kg per dose). For continuous dosing in mice, an osmotic minipump (Alzet, model 1007D) was implanted in a subcutaneous interscapular pocket. Pumps were filled with vehicle only or POL5551 to deliver the compound at a dose of 8 mg/kg/d for up to 7 d.

Mice

C57BL/6NCrl wild-type (WT) mice were purchased from Charles River. DERE_G (depletion of regulatory T cell) mice express a simian diphtheria toxin (DT) receptor-enhanced green fluorescent protein (eGFP) fusion protein under the control of the endogenous forkhead box P3 (Foxp3) promoter/enhancer region on a bacterial artificial chromosome transgene. The transcription factor Foxp3 is highly restricted to T_{reg} cells and confers immunosuppressive functions to naïve T cells.^{24,25} In DERE_G mice, DT receptor-eGFP expression is observed in fully functional CD4⁺ Foxp3⁺ T_{reg} cells, thereby allowing their DT-induced ablation or fluorescent detection. To deplete Foxp3⁺ T_{reg} cells, mice were intraperitoneally (i.p.) injected with DT (Merck, catalog number [#] 322326, 25 ng/g body weight) immediately before and 24 h after MI.²⁶ DT-treated WT littermates served as controls. Recombination activating gene 1 (*Rag1*) deficient (knockout, KO) mice which do not produce mature T and B cells, CD11c-Cre mice which express Cre recombinase under the control of the CD11c promoter/enhancer region, iDTR mice in which Cre-mediated excision of a STOP cassette renders cells sensitive to DT, and Tie2-GFP mice which express GFP under the control of the murine endothelium-specific Tie2 promoter were purchased from the Jackson Laboratory. To deplete CD11c⁺ dendritic cells (DCs),

CD11c-Cre iDTR mice were i.p. injected with DT (50 ng/g body weight) 24 h and immediately before MI.²⁷

Mouse model of reperfused acute MI

All procedures in mice were approved by the authorities in Hannover, Germany (Niedersächsisches Landesamt für Verbraucherschutz und Lebensmittelsicherheit). MI was induced in 8–10-week-old male mice by transient left anterior descending coronary artery (LAD) ligation. In sham-operated control mice, the ligature around the LAD was not tied. LV end-diastolic area (LVEDA) and LV end-systolic area (LVESA) were recorded by high-resolution 2-dimensional transthoracic echocardiography. Fractional area change (%) was calculated as $[(LVEDA - LVESA) / LVEDA] \times 100$. LV pressure-volume loops were recorded with a micromanometer-tipped conductance catheter.

Splenectomy

Mice were s.c. injected with 2 mg/kg butorphanol and anesthetized with 2% isoflurane via face mask. The abdominal cavity was entered through a small incision under the left rib cage, splenic vessels were cauterized, and the spleen was removed. In control mice, the abdomen was opened, but the spleen was left *in situ* (laparotomy only).

Adoptive splenic mononuclear cell (MNC) transfer

Spleens were aseptically removed from donor mice and placed in DMEM (Thermo Fisher Scientific). Splenocyte suspensions were prepared by carefully mincing the spleen with the plunger tip of a 1 mL syringe while passing the tissue through a 100 μ m cell strainer (BD Biosciences). Erythrocytes were depleted by NH_4Cl lysis. Cells were suspended in DMEM, layered onto Ficoll-Paque (GE Healthcare), and centrifuged for 20 min at 2,000 g at room temperature. Splenic MNCs were collected from the buffy coat and washed with PBS. Splenic

MNCs from mice belonging to the same experimental group were pooled and suspended in PBS. Cells were injected via a jugular vein catheter into splenectomized recipient mice (1.7×10^7 MNCs per mouse, corresponding to the average number of MNCs isolated from one donor mouse).

Adoptive splenic monocyte transfer

Splenic monocytes were prepared from splenic MNCs with a kit from Miltenyi Biotec (#130-100-629). In brief, highly pure untouched monocytes were isolated by depleting non-target cells (T cells, B cells, NK cells, dendritic cells, erythroid cells, and granulocytes) using magnetic cell labeling and separation (MACS). Monocytes from mice belonging to the same experimental group were pooled, suspended in PBS, and infused via a jugular vein catheter into splenectomized recipient mice (1×10^6 monocytes per mouse, corresponding to the average number of monocytes isolated from one donor mouse).

Inflammatory cell isolation

Peripheral blood was drawn from the right ventricle. Splenocyte suspensions were prepared with a gentleMACS dissociator (Miltenyi Biotec). Blood and spleen erythrocytes were depleted by NH_4Cl lysis. Inflammatory cells were isolated from the infarcted region of the left ventricle by enzymatic digestion and mechanical dissociation with a gentleMACS dissociator.

T_{reg} cell quantification and isolation

Inflammatory cells were isolated from DERE mice, incubated with a CD16/CD32 antibody (clone 2.4G2, mouse BD Fc Block, BD Biosciences) (dilution 1:100), and stained with a CD4-APC antibody (clone RM4-5, BioLegend) (dilution 1:100). $\text{CD4}^+ \text{Foxp3}^+/\text{eGFP}^+$ T_{reg} cells were counted by flow cytometry. For cell transfer experiments, $\text{CD4}^+ \text{Foxp3}^+/\text{eGFP}^+$ T_{reg} cells were isolated by FACS using a FACS Aria IIu instrument (Becton Dickinson) and infused via a jugular

vein catheter into splenectomized recipient mice (2×10^5 T_{reg} cells per mouse, corresponding to the average number of T_{reg} cells isolated from one donor mouse).

Closed-chest model of reperfused MI and magnetic resonance imaging (MRI) in pigs

All procedures in pigs were approved by the Animal Ethics Committee of the Hungarian National Food Chain Safety Office (approval number: 23.1./02322/009/2008). Acute MI was induced in domestic (DanBred hybrid) female pigs by percutaneous balloon occlusion of the mid LAD as previously described by our group.²⁸ 3 d and 6 weeks after MI, LV end-diastolic and end-systolic volumes (LVEDV and LVESV) and infarct volume were determined by contrast-enhanced MRI. LV ejection fraction (LVEF) (%) was calculated as $[(LVEDV - LVESV) / LVEDV] \times 100$. LV myocardium showing late contrast enhancement was quantified to assess infarct volume.

Statistical analyses

We randomly allocated mouse littermates and pigs to the different experimental groups. Whenever possible, the investigators were blinded to group allocation during the experiment and when assessing the outcome. No animals were excluded from the analyses. Based on visual inspection, data were normally distributed with similar variances in the different groups. With small sample sizes we did not apply statistical tests for normality or equality of variances. Data are presented as mean \pm s.e.m. unless otherwise stated. The 2-independent-sample *t* test was used to compare two groups. For comparisons among more than two groups, 1-way ANOVA was used if there was one independent variable and 2-way ANOVA if there were two independent variables. The Dunnett post hoc test was used for multiple comparisons with a single control group. The Tukey post hoc test was used to adjust for multiple comparisons. In the pig study, we used analysis of covariance (ANCOVA) to compare LVEF changes within (3 d to 6 weeks) and

between treatment groups (placebo vs. POL6326), with treatment group as the main factor and LVEF at 3 d as a covariate. Differences in least-squares means and corresponding 95% CI were calculated based on the ANCOVA model. Other endpoints were analyzed using the same methods. We considered a 2-tailed P value less than 0.05 to indicate statistical significance. K.C.W. had full access to all the data in the study and takes responsibility for the integrity of the data and the data analysis.

Results

POL5551 promotes tissue repair and improves heart function after MI

To explore the therapeutic potential of POL5551 after MI, we subjected mice to transient coronary artery ligation. This model simulates the situation in patients with acute MI receiving reperfusion therapy and was used throughout the present study. 2, 4, 6, and 8 d after MI, mice were injected intraperitoneally with POL5551 or vehicle (0.9% NaCl) only (Figure 1A). Each POL5551 bolus injection was followed by a rapid (within 2 h) mobilization of neutrophils, monocytes, and lymphocytes into the peripheral blood (Figure 1B). Cell numbers returned to baseline levels within 24 h after each injection (Figure 1B). Ly6C^{high} and Ly6C^{low} monocyte populations showed similar mobilization kinetics (Supplemental Figure I). As compared to vehicle only-treated control mice, treatment with POL5551 enhanced the number of proliferating Ki67⁺ IB4⁺ endothelial cells in the infarct border-zone at 3 d after MI (Figure 1C). This angiogenic effect was associated with more perfused capillaries at 7 d (Figure 1D) and an increase in total capillary density in the infarct border-zone at 3, 7, and 28 d (Figure 1E). POL5551 is a highly selective CXCR4 antagonist with no C-X-C motif chemokine receptor 7 (CXCR7) agonistic activity (Supplemental Figure II). POL5551 did not directly act on

endothelial cells, as has been reported for TC14012,²⁹ a combined CXCR4 antagonist and CXCR7 agonist (Figure 1F and Supplemental Figure III). POL5551-treated mice developed smaller infarct scars (Figure 1G) and less pronounced LV remodeling and systolic and diastolic dysfunction as shown by echocardiography and pressure-volume measurements (Figure 1H and 1I and Supplemental Table I).

Splenic mononuclear cells are required and sufficient for the treatment effects of POL5551

After MI, the spleen continuously supplies neutrophils and monocytes via the bloodstream to satisfy the high demand for these cells at the site of inflammation.^{30,31} To delineate the importance of specific cell subsets for the beneficial effects of intermittent CXCR4 blockade, we reassessed the therapeutic potential of POL5551 in splenectomized mice. Mice underwent splenectomy 2 d after MI, before the first injection of either POL5551 or vehicle only (Figure 2A). POL5551 did not enhance capillary density in the infarct border-zone (Figure 2B), did not reduce infarct scar size (Figure 2C), and did not attenuate LV remodeling and systolic or diastolic dysfunction in splenectomized mice (Figure 2D and 2E and Supplemental Table II), thereby indicating that the spleen is required for its therapeutic effects. POL5551's treatment effects were not affected in infarcted mice that had undergone laparotomy only 2 d after MI (data not shown).

We next explored whether splenic MNCs from POL5551-treated mice can transfer the therapeutic effects into untreated mice. Sham or MI surgeries were performed in donor mice (Figure 3A). After 2 d, donor mice were treated with POL5551 or vehicle only, and splenic MNCs, consisting mainly of lymphocytes and monocytes (Supplemental Figure IV), were prepared 24 h later. 2 d after undergoing MI surgery, recipient mice were splenectomized and then infused with donor MNCs. Capillary density in the infarct border-zone was greater in mice

that had received MNCs from POL5551-treated infarcted donors than in mice that had received MNCs from vehicle only-treated infarcted donors (Figure 3B). MNCs from POL5551-treated infarcted donors also reduced infarct scar size (Figure 3C) and attenuated LV remodeling and systolic and diastolic dysfunction in recipient mice (Figure 3D and 3E and Supplemental Table III). MNCs from sham-operated donors did not exert any therapeutic effects regardless of whether the donors had been treated with POL5551 or vehicle only (Figure 3B through 3E).

Considering the key role of splenic monocytes in orchestrating inflammation and repair after their relocation to the infarcted myocardium,^{30,31} we repeated the previous experiment and transplanted only MACS-enriched splenic monocytes from POL5551-treated infarcted donor mice into infarcted and splenectomized recipient mice (Figure 3F and Supplemental Figure IV). To our surprise, adoptively transferring splenic monocytes from POL5551-treated infarcted donors did not attenuate LV remodeling and systolic dysfunction in recipient mice (Figure 3G and 3H).

Splenic T_{reg} cells mediate the treatment effects of POL5551

The above adoptive cell transfer experiments pointed to splenic lymphocytes as potential mediators of POL5551's treatment effects. To address this hypothesis, we induced MI in *Rag1* KO mice and their WT littermates and treated the animals with POL5551 or vehicle only. POL5551 attenuated adverse LV remodeling and systolic dysfunction in *Rag1* WT but not *Rag1* KO mice, indicating that T and/or B cells are required for the treatment effects (Supplemental Figure V).

Recent studies have implicated T_{reg} cells in promoting tissue repair and functional recovery after MI.³²⁻³⁵ We therefore repeated the experiment in T_{reg} cell-depleted DERE mice. DERE mice were injected with DT or saline immediately before and 24 h after MI. Treatment with

POL5551 or vehicle only was started 2 d after MI (Figure 4A). DT efficiently depleted CD4⁺ Foxp3⁺/eGFP⁺ T_{reg} cells in DERE mice (Figure 4B). POL5551 enhanced the capillary density in the infarct border-zone (Figure 4C), reduced infarct scar size (Figure 4D), and ameliorated adverse remodeling and systolic dysfunction (Figure 4E and 4F and Supplemental Table IV) in saline-injected, non-T_{reg} cell-depleted DERE mice. T_{reg} cell depletion, however, completely abolished the treatment effects of POL5551 (Figure 4C through 4F and Supplemental Table IV). POL5551's treatment effects were not affected in DT-treated WT mice (Supplemental Figure VI).

To further examine the importance of T_{reg} cells for the therapeutic effects of CXCR4 blockade, we performed adoptive splenic MNC transfer experiments using T_{reg} cell-depleted or non-T_{reg} cell-depleted DERE mice as donors and WT mice as recipients (Figure 5A). MI was induced in donor and recipient mice. Donor mice were injected with DT or saline immediately before and 24 h after MI. 2 d after MI, donor mice were treated with POL5551, and splenic MNCs were prepared 24 h later. 2 d after MI, recipient mice were splenectomized and then infused with donor MNCs (Figure 5A). Capillary density in the infarct border-zone was greater (Figure 5B), infarct scar size was smaller (Figure 5C), and postinfarction LV remodeling (Figure 5D) and systolic dysfunction (Figure 5E) were less severe in recipient mice transplanted with non-T_{reg} cell-depleted MNCs compared with mice that were transplanted with T_{reg} cell-depleted MNCs. These findings further supported our conclusion that splenic T_{reg} cells are required for POL5551's treatment effects.

Next, we explored whether POL5551-primed splenic T_{reg} cells are also sufficient to promote tissue repair and functional recovery after MI. To this end, MI was induced in DERE donor and WT recipient mice. 2 d after MI, donor mice were treated with POL5551 or vehicle only. Splenic

CD4⁺ Foxp3⁺/eGFP⁺ T_{reg} cells were prepared 24 h later (Figure 5F and 5G). 2 d after MI, recipient mice were splenectomized and then infused with donor T_{reg} cells (Figure 5F). Capillary density in the infarct border-zone was greater (Figure 5H), infarct scar size was smaller (Figure 5I), and postinfarction LV remodeling (Figure 5J) and systolic dysfunction (Figure 5K) were less severe in recipient mice transplanted with T_{reg} cells from POL5551-treated donors compared with mice that were transplanted with T_{reg} cells from vehicle only-treated donors.

Dendritic cells are required for POL5551's treatment effects

The MNC transfer experiments shown in Figure 3A through 3E indicated that instructive cues provided by the infarct are required for POL5551's treatment effects. MI has recently been shown to prime DCs which in turn promote T_{reg} cell activation.³⁶ We therefore performed adoptive splenic MNC transfer experiments using DC-depleted or non-DC-depleted CD11c-Cre iDTR infarcted mice as donors and infarcted WT mice as recipients (Figure 5L). Donor mice were injected with DT or saline 24 h and immediately before MI. 2 d after MI, donor mice were treated with POL5551, and splenic MNCs were prepared 24 h later (Figure 5M). 2 d after MI, recipient mice were splenectomized and then infused with donor MNCs (Figure 5L). Capillary density in the infarct border-zone was greater (Figure 5N), infarct scar size was smaller (Figure 5O), and postinfarction LV remodeling (Figure 5P) and systolic dysfunction (Figure 5Q) were less severe in recipient mice transplanted with MNCs from non-DC-depleted donors compared with mice that were transplanted with MNCs from DC-depleted donors.

POL5551 enhances T_{reg} cell mobilization, cardiac recruitment, and immune-regulatory function

We treated infarcted DERE mice with POL5551 or vehicle only and quantified CD4⁺ Foxp3⁺/eGFP⁺ T_{reg} cells in the circulation and the infarcted left ventricle by flow cytometry.

Each POL5551 injection was followed by rapid T_{reg} cell mobilization into the peripheral blood (Figure 6A). T_{reg} cell mobilization displayed similar kinetics to other inflammatory cell populations (Figure 1B) and was paralleled by enhanced T_{reg} cell accumulation in the infarcted left ventricle (Figure 6B). Enhanced T_{reg} cell recruitment was confined to the infarcted region (Figure 6C). In both vehicle only- and POL5551-treated mice, between 87 and 96% of CD4⁺ Foxp3⁺/eGFP⁺ T_{reg} cells in the infarcted left ventricle (both in the infarcted and noninfarcted regions) expressed the activation marker CD69 antigen (5 mice per group, P=n.s.). POL5551 did not increase neutrophil, monocyte or macrophage (Ly6C^{high} and Ly6C^{low}), or total lymphocyte accumulation in the infarcted region (Supplemental Figure VII). Circulating T_{reg} cell numbers were much lower in infarcted mice that had undergone splenectomy before POL5551 injection (Figure 6D), pointing to the spleen as the main T_{reg} cell reservoir. Indeed, POL5551 did not enhance T_{reg} cell accumulation in the infarcted region in splenectomized mice (Figure 6E).

The cell transfer experiments shown in Figure 5F through 5K, where we had transplanted equal numbers of splenic CD4⁺ Foxp3⁺/eGFP⁺ T_{reg} cells from POL5551- and vehicle only-treated donors, indicated that POL5551 also enhances T_{reg} cell functionality. We therefore explored if POL5551 enhances T_{reg} cells' capacity to home to the infarct. Indeed, T_{reg} cell recruitment to the infarcted region was greater in mice that had been transplanted with T_{reg} cells from POL5551-treated donors than in mice that had been transplanted with equal numbers of T_{reg} cells from vehicle only-treated donors (Figure 6F). T_{reg} cells from POL5551-treated donors also showed a somewhat greater activity in T_{reg} cell suppression assays (Supplemental Figure VIII). Expression of T cell activation markers on T_{reg} cells from POL5551- or vehicle only-treated donors did not differ significantly (Supplemental Table V).

We next explored whether POL5551 modulates gene expression in myeloid cells and

whether T_{reg} cells may be involved. DERE mice were injected with either DT or saline immediately before and 1 d after MI. 2 d after MI, mice were treated with POL5551 or vehicle only. Ly6C^{low/high} monocytes and macrophages were isolated from the infarcted region 2 d later and used for RT-qPCR analyses. POL5551 attenuated the expression of tumor necrosis factor (TNF), interleukin 1 β (IL-1 β), interferon γ (IFN- γ), and nitric oxide synthase 2 (NOS2) in Ly6C^{low/high} monocytes and macrophages in non-T_{reg} cell-depleted but not in T_{reg} cell-depleted DERE mice (Figure 6G). Expression levels of interleukin 10 (IL-10) and transforming growth factor β 1 (TGF- β 1) were not altered by POL5551 (Figure 6G).

Continuous POL5551 infusion mobilizes T_{reg} cells but prevents their cardiac recruitment and therapeutic effects



Consistent with previous reports,^{15,16} CXCL12 expression was significantly increased in the infarcted region, peaking at 7 d and returning to baseline levels at 28 d (Figure 7A). To assess the importance of CXCL12 for T_{reg} cell recruitment to the infarcted region, we treated infarcted DERE mice with POL5551 bolus injections as before or with a continuous POL5551 infusion starting 2 d after MI (Figure 7B). Bolus injections and continuous POL5551 infusion both mobilized CD4⁺ Foxp3⁺/eGFP⁺ T_{reg} cells into the circulation (Figure 7C). Continuous POL5551 infusion, however, prevented T_{reg} cell recruitment to the infarcted region (Figure 7D). In a related experiment, we treated infarcted WT mice with POL5551 bolus injections or with a continuous POL5551 infusion (Figure 7E). Unlike the bolus injections, continuous POL5551 infusion did not enhance infarct border-zone capillarization (Figure 7F), did not reduce infarct scar size (Figure 7G), and did not attenuate LV remodeling and systolic dysfunction (Figure 7H and 7I).

POL6326 treatment effects in pigs with reperfused acute MI

We treated pigs with reperfused acute MI with POL6326 to explore the translational potential of CXCR4 blockade with a peptidic macrocycle antagonist. Like POL5551, POL6326 mobilized T_{reg} cells, enhanced T_{reg} cell recruitment to the infarct, attenuated TNF expression in monocytes and macrophages in the infarcted region, enhanced infarct border-zone capillarization, reduced infarct scar size, and attenuated LV remodeling and systolic dysfunction in mice (Supplemental Figure IX). 4, 6, 8, and 10 d after MI, pigs were infused intravenously with the clinical stage compound POL6326 or vehicle only. Contrast-enhanced cardiac MRI was performed 3 d and 6 weeks after MI (Table). Infarct volume decreased, on average, by 1.6 mL in the control group (P=0.28) and by 6.2 mL in the POL6326 group (P<0.001), corresponding to a POL6326 treatment effect of -4.6 mL (P=0.035). Increases in LVEDV and LVESV over time tended to be more pronounced in the control group than in the POL6326 group. Mean LVEF decreased by 2.1 percentage points in the control group (P=0.19) and increased by 3.1 percentage points in the POL6326 group (P=0.06), corresponding to a POL6326 treatment effect of 5.2 percentage points (P=0.027).

Discussion

Patients who develop heart failure after MI remain at high risk of death and frequent hospitalizations.³⁷ Available strategies to prevent postinfarction heart failure aim at limiting ischemic injury and chronic LV remodeling.³⁸ Infarct healing may afford an additional time window of therapeutic opportunity wherein transient interventions can have a lasting impact on cardiac function.⁴ In the present study, repeated bolus application of POL5551, a highly selective peptidic macrocycle CXCR4 antagonist, promoted angiogenesis and tissue repair, and attenuated

LV remodeling and systolic and diastolic dysfunction in a mouse model of reperfused acute MI. As shown by a series of cell depletion and transfer experiments, splenic CD4⁺ Foxp3⁺ T_{reg} cells mediated these therapeutic effects.

T_{reg} cells are a subpopulation of CD4⁺ T cells that maintain immune homeostasis by controlling adaptive and innate immune responses at multiple levels. Dysregulated T_{reg} cell generation or function has been implicated in autoimmunity, cancer, and cardiovascular disease.³⁹ CXCR4 is expressed on T_{reg} cells and other lymphocyte populations.⁴⁰ Of note, CXCR4 was originally discovered as a coreceptor for the entry of human immunodeficiency virus into CD4⁺ T cells, and the CXCR4 antagonist plerixafor was first developed as an antiviral agent.⁴¹ During the initial pharmacodynamic studies, marked increases in peripheral white blood cell counts were observed after systemic injections of plerixafor, with lymphocytes representing one component of this generalized leukocytosis.⁴² In fact, plerixafor mobilizes T cells (including T_{reg} cells) and B cells more efficiently than granulocyte-colony stimulating factor.⁴⁰ Consistent with this earlier report, POL5551 led to a rapid mobilization of Foxp3⁺ T_{reg} cells in our study. Within 24 h after each POL5551 injection, Foxp3⁺ T_{reg} cell numbers in the circulation returned to baseline levels, consistent with T_{reg} cell redistribution into tissues after the interruption of the CXCR4/CXCL12 interaction had ended due to rapid clearance of the drug.²¹ POL5551 enhanced cardiac recruitment of Foxp3⁺ T_{reg} cells, indicating that some of the mobilized Foxp3⁺ T_{reg} cells homed to the infarcted myocardium. Neutrophils, Ly6C^{high} and Ly6C^{low} monocytes, and lymphocytes displayed similar mobilization kinetics after POL5551 injections, but cardiac recruitment of these cells did not increase. Notably, continuous infusion of POL5551 prevented mobilized T_{reg} cell homing to the CXCL12-expressing infarcted region and did not promote tissue repair and functional recovery. This indicates that T_{reg} cells are recruited to the infarcted

region via the CXCR4/CXCL12 axis (not excluding the involvement of additional chemokines)⁷ and reconciles our findings with reports from the cancer field that show that continuous CXCR4 blockade inhibits T_{reg} cell homing to CXCL12-expressing tumors.^{43,44}

CXCL12/CXCR4 signals are critical for T_{reg} cell trafficking between the bone marrow and the periphery.⁴⁵ Other anatomic niches harboring T_{reg} cells via CXCR4/CXCL12 interactions remain poorly defined. In our study, Foxp3⁺ T_{reg} cell mobilization was strongly reduced in splenectomized mice pointing to the spleen as the main Foxp3⁺ T_{reg} cell reservoir amenable to POL5551-mediated mobilization. Splenectomy also abolished POL5551's effects on T_{reg} cell recruitment to the infarct, infarct border-zone angiogenesis, scar size, and LV remodeling. Likewise, depleting mature T and B cells in *Rag1* KO mice or specifically depleting Foxp3⁺ T_{reg} cells in DEREK mice eliminated POL5551's therapeutic effects. Adoptive cell transfer experiments using splenic MNCs, Foxp3⁺ T_{reg} cell-depleted splenic MNCs, or splenic Foxp3⁺ T_{reg} cells from POL5551-treated infarcted donor mice confirmed splenic Foxp3⁺ T_{reg} cells as the prime mediators of POL5551's treatment effects.

Splenic MNC transfer experiments comparing infarcted vs. noninfarcted and DC-depleted vs. non-DC-depleted donor mice revealed that instructive cues provided by the infarct – specifically by DCs – are required for POL5551's treatment effects. Considering that Foxp3⁺ T_{reg} cells are the splenic MNC population mediating POL5551's treatment effects, and that infarcted myocardium-primed DCs promote T_{reg} cell expansion and activation,³⁶ we conclude that MI-primed DCs are required to render T_{reg} cells responsive to POL5551.

Expanding the circulating T_{reg} cell pool by adoptive T_{reg} cell transfer or treatment with a superagonistic anti-CD28 antibody enhances T_{reg} cell recruitment to the infarcted region, improves wound healing, and attenuates LV remodeling in mice and rats with acute MI.³²⁻³⁴

POL5551's therapeutic effects may therefore relate in part to increased T_{reg} cell availability. Adoptive T_{reg} cell transfer experiments indicated that POL5551 in addition enhances T_{reg} cell functionality. Specifically, POL5551 increased T_{reg} cells' capacity to home to the infarct and (slightly) promoted T_{reg} cell immunosuppressive function.

Acute MI activates autoreactive CD4⁺ T cells,^{46,47} that may trigger autoimmune damage to the myocardium in mice and possibly patients with type 1 diabetes.⁴⁸ Postinfarction autoimmune injury, however, is usually not observed in nondiabetic mice.^{47,48} Suppression of autoimmune injury may therefore not be the prime mechanism whereby T_{reg} cell mobilization or T_{reg} cell expansion³²⁻³⁴ promote therapeutic effects after MI. Instead, T_{reg} cells have been proposed to modulate innate immune responses after MI at multiple levels.^{34,35} T_{reg} cell depletion before the infarct may lead to higher monocyte and macrophage accumulation in the infarcted region.^{34,35}

Still, treatment with POL5551, starting 2 d after MI, did not affect monocyte and macrophage numbers in the infarcted myocardium. Similarly, treatment with an anti-CD28 antibody 2 d after MI did not affect monocyte and macrophage accumulation,³⁴ indicating that timing may be important and/or that endogenous T_{reg} cell effects on innate immune cell recruitment cannot be further enhanced by these interventions. T_{reg} cells have also been shown to modulate inflammatory gene expression in monocytes and macrophages in the infarcted myocardium.³⁴ Consistently, we found that POL5551, via Foxp3⁺ T_{reg} cells, attenuated the expression of TNF, IL-1 β , IFN- γ , and NOS2 in monocytes and macrophages in the infarcted region.

In conclusion, our data confirm CXCR4 blockade as a promising treatment strategy to enhance tissue repair and functional recovery after acute MI.¹⁰⁻¹² We identify CD4⁺ Foxp3⁺ T_{reg} cells as the central arbiters of these therapeutic effects and thereby delineate a new pharmacological strategy to acutely and transiently augment T_{reg} cell function *in vivo*.⁴⁹

Highlighting the translational potential of this approach, the clinical-stage compound POL6326 reduced infarct volume and promoted LVEF recovery in a porcine closed-chest model of reperfused acute MI.⁵⁰ These findings should stimulate further research into the therapeutic potential of CXCR4 antagonists after MI and in other acute conditions wherein excessive innate and/or adaptive immune responses cause immunopathology.

Acknowledgments

The authors are grateful to Dr. Matthias Ballmaier from the FACS core facility and Dr. Christine S. Falk from the Institute of Transplant Immunology at Hannover Medical School for support with cell sorting.



Sources of Funding

This study was supported by grants from the German Research Foundation (WO 552/9-2, WO 552/10-1, and Excellence Cluster Von Regenerativer Biologie zu Rekonstruktiver Therapie 2 [REBIRTH-2] to Dr. Wollert). Polyphor (Allschwil, Switzerland) provided financial support.

Disclosures

Drs. Chevalier and Dembowsky were employees of Polyphor during experiments and manuscript preparation. The other authors report no conflicts.

References

1. Bagai A, Dangas GD, Stone GW, Granger CB. Reperfusion strategies in acute coronary syndromes. *Circ Res*. 2014;114:1918-1928. doi: 10.1161/CIRCRESAHA.114.302744.
2. Stone GW, Selker HP, Thiele H, Patel MR, Udelson JE, Ohman EM, Maehara A, Eitel I, Granger CB, Jenkins PL, Nichols M, Ben-Yehuda O. Relationship between infarct size and outcomes following primary PCI: Patient-level analysis from 10 randomized trials. *J Am Coll Cardiol*. 2016;67:1674-1683. doi: 10.1016/j.jacc.2016.01.069.
3. Westman PC, Lipinski MJ, Luger D, Waksman R, Bonow RO, Wu E, Epstein SE. Inflammation as a driver of adverse left ventricular remodeling after acute myocardial infarction. *J Am Coll Cardiol*. 2016;67:2050-2060. doi: 10.1016/j.jacc.2016.01.073.
4. Prabhu SD, Frangogiannis NG. The biological basis for cardiac repair after myocardial infarction: From inflammation to fibrosis. *Circ Res*. 2016;119:91-112. doi: 10.1161/CIRCRESAHA.116.303577.
5. Nourshargh S, Alon R. Leukocyte migration into inflamed tissues. *Immunity*. 2014;41:694-707. doi: 10.1016/j.immuni.2014.10.008.
6. Dewald O, Zymek P, Winkelmann K, Koerting A, Ren G, Abou-Khamis T, Michael LH, Rollins BJ, Entman ML, Frangogiannis NG. CCL2/monocyte chemoattractant protein-1 regulates inflammatory responses critical to healing myocardial infarcts. *Circ Res*. 2005;96:881-889. doi: 10.1161/01.RES.0000163017.13772.3a.
7. Dobaczewski M, Xia Y, Bujak M, Gonzalez-Quesada C, Frangogiannis NG. CCR5 signaling suppresses inflammation and reduces adverse remodeling of the infarcted heart, mediating recruitment of regulatory T cells. *Am J Pathol*. 2010;176:2177-2187. doi: 10.2353/ajpath.2010.090759.
8. Anzai A, Choi JL, He S, Fenn AM, Nairz M, Rattik S, McAlpine CS, Mindur JE, Chan CT, Iwamoto Y, Tricot B, Wojtkiewicz GR, Weissleder R, Libby P, Nahrendorf M, Stone JR, Becher B, Swirski FK. The infarcted myocardium solicits GM-CSF for the detrimental oversupply of inflammatory leukocytes. *J Exp Med*. 2017;214:3293-3310. doi: 10.1084/jem.20170689.
9. Majmudar MD, Keliher EJ, Heidt T, Leuschner F, Truelove J, Sena BF, Gorbato R, Iwamoto Y, Dutta P, Wojtkiewicz G, Courties G, Sebas M, Borodovsky A, Fitzgerald K, Nolte MW, Dickneite G, Chen JW, Anderson DG, Swirski FK, Weissleder R, Nahrendorf M. Monocyte-directed RNAi targeting CCR2 improves infarct healing in atherosclerosis-prone mice. *Circulation*. 2013;127:2038-2046. doi: 10.1161/CIRCULATIONAHA.112.000116.
10. Jujo K, Hamada H, Iwakura A, Thorne T, Sekiguchi H, Clarke T, Ito A, Misener S, Tanaka T, Klyachko E, Kobayashi K, Tongers J, Roncalli J, Tsurumi Y, Hagiwara N, Losordo DW. CXCR4 blockade augments bone marrow progenitor cell recruitment to the neovasculature and reduces mortality after myocardial infarction. *Proc Natl Acad Sci U S A*. 2010;107:11008-11013. doi: 10.1073/pnas.0914248107.
11. Jujo K, Ii M, Sekiguchi H, Klyachko E, Misener S, Tanaka T, Tongers J, Roncalli J, Renault MA, Thorne T, Ito A, Clarke T, Kamide C, Tsurumi Y, Hagiwara N, Qin G, Asahi M, Losordo DW. CXC-chemokine receptor 4 antagonist AMD3100 promotes cardiac functional recovery after ischemia/reperfusion injury via endothelial nitric oxide synthase-dependent mechanism. *Circulation*. 2013;127:63-73. doi: 10.1161/CIRCULATIONAHA.112.099242.
12. Hsu WT, Jui HY, Huang YH, Su MY, Wu YW, Tseng WY, Hsu MC, Chiang BL, Wu KK, Lee CM. CXCR4 antagonist TG-0054 mobilizes mesenchymal stem cells, attenuates

- inflammation, and preserves cardiac systolic function in a porcine model of myocardial infarction. *Cell Transplant*. 2015;24:1313-1328. doi: 10.3727/096368914X681739.
13. Broxmeyer HE, Orschell CM, Clapp DW, Hangoc G, Cooper S, Plett PA, Liles WC, Li X, Graham-Evans B, Campbell TB, Calandra G, Bridger G, Dale DC, Srouf EF. Rapid mobilization of murine and human hematopoietic stem and progenitor cells with AMD3100, a CXCR4 antagonist. *J Exp Med*. 2005;201:1307-1318. doi: 10.1084/jem.20041385.
 14. Karpova D, Bonig H. Concise review: CXCR4/CXCL12 signaling in immature hematopoiesis: Lessons from pharmacological and genetic models. *Stem Cells*. 2015;33:2391-2399. doi: 10.1002/stem.2054.
 15. Askari AT, Unzek S, Popovic ZB, Goldman CK, Forudi F, Kiedrowski M, Rovner A, Ellis SG, Thomas JD, DiCorleto PE, Topol EJ, Penn MS. Effect of stromal-cell-derived factor 1 on stem-cell homing and tissue regeneration in ischaemic cardiomyopathy. *Lancet*. 2003;362:697-703. doi: 10.1016/S0140-6736(03)14232-8.
 16. Abbott JD, Huang Y, Liu D, Hickey R, Krause DS, Giordano FJ. Stromal cell-derived factor-1 α plays a critical role in stem cell recruitment to the heart after myocardial infarction but is not sufficient to induce homing in the absence of injury. *Circulation*. 2004;110:3300-3305. doi: 10.1161/01.CIR.0000147780.30124.CF.
 17. Segers VF, Tokunou T, Higgins LJ, MacGillivray C, Gannon J, Lee RT. Local delivery of protease-resistant stromal cell derived factor-1 for stem cell recruitment after myocardial infarction. *Circulation*. 2007;116:1683-1692. doi: 10.1161/CIRCULATIONAHA.107.718718.
 18. Fadini GP, Losordo D, Dimmeler S. Critical reevaluation of endothelial progenitor cell phenotypes for therapeutic and diagnostic use. *Circ Res*. 2012;110:624-637. doi: 10.1161/CIRCRESAHA.111.243386.
 19. Loetscher M, Geiser T, O'Reilly T, Zwahlen R, Baggiolini M, Moser B. Cloning of a human seven-transmembrane domain receptor, LESTR, that is highly expressed in leukocytes. *J Biol Chem*. 1994;269:232-237.
 20. Rettig MP, Anstas G, DiPersio JF. Mobilization of hematopoietic stem and progenitor cells using inhibitors of CXCR4 and VLA-4. *Leukemia*. 2012;26:34-53. doi: 10.1038/leu.2011.197.
 21. Karpova D, Dauber K, Spohn G, Chudziak D, Wiercinska E, Schulz M, Pettit AR, Levesque JP, Romagnoli B, Patel K, Chevalier E, Dembowski K, Bonig H. The novel CXCR4 antagonist POL5551 mobilizes hematopoietic stem and progenitor cells with greater efficiency than plerixafor. *Leukemia*. 2013;27:2322-2331. doi: 10.1038/leu.2013.266.
 22. Karpova D, Brauning S, Wiercinska E, Kramer A, Stock B, Graff J, Martin H, Wach A, Escot C, Douglas G, Romagnoli B, Chevalier E, Dembowski K, Hooftman L, Bonig H. Mobilization of hematopoietic stem cells with the novel CXCR4 antagonist POL6326 (balixafortide) in healthy volunteers-results of a dose escalation trial. *J Transl Med*. 2017;15:2. doi: 10.1186/s12967-016-1107-2.
 23. Luther A, Moehle K, Chevalier E, Dale G, Obrecht D. Protein epitope mimetic macrocycles as biopharmaceuticals. *Curr Opin Chem Biol*. 2017;38:45-51. doi: 10.1016/j.cbpa.2017.02.004.
 24. Chen W, Jin W, Hardegen N, Lei KJ, Li L, Marinos N, McGrady G, Wahl SM. Conversion of peripheral CD4⁺CD25⁻ naive T cells to CD4⁺CD25⁺ regulatory T cells by TGF- β induction of transcription factor Foxp3. *J Exp Med*. 2003;198:1875-1886. doi: 10.1084/jem.20030152.

25. Hori S, Nomura T, Sakaguchi S. Control of regulatory T cell development by the transcription factor Foxp3. *Science*. 2003;299:1057-1061. doi: 10.1126/science.1079490.
26. Lahl K, Sparwasser T. In vivo depletion of FoxP3⁺ Tregs using the DERE mouse model. *Methods Mol Biol*. 2011;707:157-172. doi: 10.1007/978-1-61737-979-6_10.
27. Yogeve N, Frommer F, Lukas D, Kautz-Neu K, Karam K, Ielo D, von Stebut E, Probst HC, van den Broek M, Riethmacher D, Birnberg T, Blank T, Reizis B, Korn T, Wiendl H, Jung S, Prinz M, Kurschus FC, Waisman A. Dendritic cells ameliorate autoimmunity in the CNS by controlling the homeostasis of PD-1 receptor⁺ regulatory T cells. *Immunity*. 2012;37:264-275. doi: 10.1016/j.immuni.2012.05.025.
28. Baranyai T, Giricz Z, Varga ZV, Koncsos G, Lukovic D, Makkos A, Sarkozy M, Pavo N, Jakab A, Czimbalmos C, Vago H, Ruzsa Z, Toth L, Garamvolgyi R, Merkely B, Schulz R, Gyongyosi M, Ferdinandy P. In vivo MRI and ex vivo histological assessment of the cardioprotection induced by ischemic preconditioning, postconditioning and remote conditioning in a closed-chest porcine model of reperfused acute myocardial infarction: Importance of microvasculature. *J Transl Med*. 2017;15:67. doi: 10.1186/s12967-017-1166-z.
29. Hao H, Hu S, Chen H, Bu D, Zhu L, Xu C, Chu F, Huo X, Tang Y, Sun X, Ding BS, Liu DP, Hu S, Wang M. Loss of endothelial CXCR7 impairs vascular homeostasis and cardiac remodeling after myocardial infarction: Implications for cardiovascular drug discovery. *Circulation*. 2017;135:1253-1264. doi: 10.1161/CIRCULATIONAHA.116.023027.
30. Swirski FK, Nahrendorf M, Etzrodt M, Wildgruber M, Cortez-Retamozo V, Panizzi P, Figueiredo JL, Kohler RH, Chudnovskiy A, Waterman P, Aikawa E, Mempel TR, Libby P, Weissleder R, Pittet MJ. Identification of splenic reservoir monocytes and their deployment to inflammatory sites. *Science*. 2009;325:612-616. doi: 10.1126/science.1175202.
31. Leuschner F, Rauch PJ, Ueno T, Gorbato R, Marinelli B, Lee WW, Dutta P, Wei Y, Robbins C, Iwamoto Y, Sena B, Chudnovskiy A, Panizzi P, Keliher E, Higgins JM, Libby P, Moskowitz MA, Pittet MJ, Swirski FK, Weissleder R, Nahrendorf M. Rapid monocyte kinetics in acute myocardial infarction are sustained by extramedullary monocytopoiesis. *J Exp Med*. 2012;209:123-137. doi: 10.1084/jem.20111009.
32. Tang TT, Yuan J, Zhu ZF, Zhang WC, Xiao H, Xia N, Yan XX, Nie SF, Liu J, Zhou SF, Li JJ, Yao R, Liao MY, Tu X, Liao YH, Cheng X. Regulatory T cells ameliorate cardiac remodeling after myocardial infarction. *Basic Res Cardiol*. 2012;107:232. doi: 10.1007/s00395-011-0232-6.
33. Sharir R, Semo J, Shimoni S, Ben-Mordechai T, Landa-Rouben N, Maysel-Auslender S, Shaish A, Entin-Meer M, Keren G, George J. Experimental myocardial infarction induces altered regulatory T cell homeostasis, and adoptive transfer attenuates subsequent remodeling. *Plos One*. 2014;9:e113653. doi: 10.1371/journal.pone.0113653.
34. Weirather J, Hofmann UD, Beyersdorf N, Ramos GC, Vogel B, Frey A, Ertl G, Kerkau T, Frantz S. Foxp3⁺ CD4⁺ T cells improve healing after myocardial infarction by modulating monocyte/macrophage differentiation. *Circ Res*. 2014;115:55-67. doi: 10.1161/CIRCRESAHA.115.303895.
35. Saxena A, Dobaczewski M, Rai V, Haque Z, Chen W, Li N, Frangogiannis NG. Regulatory T cells are recruited in the infarcted mouse myocardium and may modulate fibroblast phenotype and function. *Am J Physiol Heart Circ Physiol*. 2014;307:H1233-H1242. doi: 10.1152/ajpheart.00328.2014.
36. Choo EH, Lee JH, Park EH, Park HE, Jung NC, Kim TH, Koh YS, Kim E, Seung KB, Park C, Hong KS, Kang K, Song JY, Seo HG, Lim DS, Chang K. Infarcted myocardium-primed

- dendritic cells improve remodeling and cardiac function after myocardial infarction by modulating the regulatory T cell and macrophage polarization. *Circulation*. 2017;135:1444-1457. doi: 10.1161/CIRCULATIONAHA.116.023106.
37. Chen J, Hsieh AF, Dharmarajan K, Masoudi FA, Krumholz HM. National trends in heart failure hospitalization after acute myocardial infarction for Medicare beneficiaries: 1998-2010. *Circulation*. 2013;128:2577-2584. doi: 10.1161/CIRCULATIONAHA.113.003668.
38. Szummer K, Wallentin L, Lindhagen L, Alfredsson J, Erlinge D, Held C, James S, Kellerth T, Lindahl B, Ravn-Fischer A, Rydberg E, Yndigegn T, Jernberg T. Improved outcomes in patients with ST-elevation myocardial infarction during the last 20 years are related to implementation of evidence-based treatments: Experiences from the SWEDEHEART registry 1995-2014. *Eur Heart J*. 2017;38:3056-3065. doi: 10.1093/eurheartj/ehx515.
39. Meng X, Yang J, Dong M, Zhang K, Tu E, Gao Q, Chen W, Zhang C, Zhang Y. Regulatory T cells in cardiovascular diseases. *Nat Rev Cardiol*. 2016;13:167-179. doi: 10.1038/nrcardio.2015.169.
40. Kean LS, Sen S, Onabajo O, Singh K, Robertson J, Stempora L, Bonifacino AC, Metzger ME, Promislow DE, Mattapallil JJ, Donahue RE. Significant mobilization of both conventional and regulatory T cells with AMD3100. *Blood*. 2011;118:6580-6590. doi: 10.1182/blood-2011-06-359331.
41. Donzella GA, Schols D, Lin SW, Este JA, Nagashima KA, Maddon PJ, Allaway GP, Sakmar TP, Henson G, De Clercq E, Moore JP. AMD3100, a small molecule inhibitor of HIV-1 entry via the CXCR4 co-receptor. *Nat Med*. 1998;4:72-77.
42. De Clercq E. The bicyclam AMD3100 story. *Nat Rev Drug Discov*. 2003;2:581-587. doi: 10.1038/nrd1134.
43. Righi E, Kashiwagi S, Yuan J, Santosuosso M, Leblanc P, Ingraham R, Forbes B, Edelblute B, Collette B, Xing D, Kowalski M, Mingari MC, Vianello F, Birrer M, Orsulic S, Dranoff G, Poznansky MC. CXCL12/CXCR4 blockade induces multimodal antitumor effects that prolong survival in an immunocompetent mouse model of ovarian cancer. *Cancer Res*. 2011;71:5522-5534. doi: 10.1158/0008-5472.CAN-10-3143.
44. Chen Y, Ramjiawan RR, Reiberger T, Ng MR, Hato T, Huang Y, Ochiai H, Kitahara S, Unan EC, Reddy TP, Fan C, Huang P, Bardeesy N, Zhu AX, Jain RK, Duda DG. CXCR4 inhibition in tumor microenvironment facilitates anti-programmed death receptor-1 immunotherapy in sorafenib-treated hepatocellular carcinoma in mice. *Hepatology*. 2015;61:1591-1602. doi: 10.1002/hep.27665.
45. Zou L, Barnett B, Safah H, Larussa VF, Evdemon-Hogan M, Mottram P, Wei S, David O, Curiel TJ, Zou W. Bone marrow is a reservoir for CD4⁺CD25⁺ regulatory T cells that traffic through CXCL12/CXCR4 signals. *Cancer Res*. 2004;64:8451-8455. doi: 10.1158/0008-5472.CAN-04-1987.
46. Van der Borgh K, Scott CL, Nindl V, Bouche A, Martens L, Sichien D, Van Moorleghe J, Vanheerswynghe M, De Prijck S, Saeys Y, Ludewig B, Gillebert T, Guillems M, Carmeliet P, Lambrecht BN. Myocardial infarction primes autoreactive T cells through activation of dendritic cells. *Cell Rep*. 2017;18:3005-3017. doi: 10.1016/j.celrep.2017.02.079.
47. Hofmann U, Beyersdorf N, Weirather J, Podolskaya A, Bauersachs J, Ertl G, Kerkau T, Frantz S. Activation of CD4⁺ T lymphocytes improves wound healing and survival after experimental myocardial infarction in mice. *Circulation*. 2012;125:1652-1663. doi: 10.1161/CIRCULATIONAHA.111.044164.

48. Gottumukkala RV, Lv H, Cornivelli L, Wagers AJ, Kwong RY, Bronson R, Stewart GC, Schulze PC, Chutkow W, Wolpert HA, Lee RT, Lipes MA. Myocardial infarction triggers chronic cardiac autoimmunity in type 1 diabetes. *Sci Transl Med*. 2012;4:138ra80. doi: 10.1126/scitranslmed.3003551.
49. Trzonkowski P, Bacchetta R, Battaglia M, Berglund D, Bohnenkamp HR, ten Brinke A, Bushell A, Cools N, Geissler EK, Gregori S, Marieke van Ham S, Hilkens C, Hutchinson JA, Lombardi G, Madrigal JA, Marek-Trzonkowska N, Martinez-Caceres EM, Roncarolo MG, Sanchez-Ramon S, Saudemont A, Sawitzki B. Hurdles in therapy with regulatory T cells. *Sci Transl Med*. 2015;7:304ps18. doi: 10.1126/scitranslmed.aaa7721.
50. van der Spoel TI, Jansen of Lorkeers SJ, Agostoni P, van Belle E, Gyongyosi M, Sluiter JP, Cramer MJ, Doevendans PA, Chamuleau SA. Human relevance of pre-clinical studies in stem cell therapy: Systematic review and meta-analysis of large animal models of ischaemic heart disease. *Cardiovasc Res*. 2011;91:649-658. doi: 10.1093/cvr/cvr113.



Circulation

Table. POL6326 treatment effects in pigs with reperfused acute myocardial infarction (MI)

	3 days (mean \pm s.e.m.)	6 weeks (mean \pm s.e.m.)	Change (mean with 95% CI)	P value	Treatment effect (mean with 95% CI)	P value
Infarct volume (mL)						
Control	18.1 \pm 2.4	17.1 \pm 1.9	-1.6 (-4.6 to 1.4)	0.28		
POL6326	20.2 \pm 1.7	13.4 \pm 1.3	-6.2 (-9.2 to -3.2)	<0.001	-4.6 (-8.8 to -0.3)	0.035
LVEDV (mL)						
Control	62.2 \pm 3.4	69.9 \pm 4.7	7.4 (-1.3 to 16.2)	0.09		
POL6326	62.7 \pm 2.2	68.0 \pm 3.6	5.5 (-3.2 to 14.2)	0.20	-1.9 (-14.2 to 10.4)	0.75
LVESV (mL)						
Control	35.1 \pm 2.7	41.2 \pm 3.9	5.7 (-1.3 to 12.8)	0.11		
POL6326	36.6 \pm 1.8	38.4 \pm 3.1	2.3 (-4.8 to 9.3)	0.52	-3.5 (-13.4 to 6.5)	0.48
LVEF (%)						
Control	44.3 \pm 2.2	41.9 \pm 2.3	-2.1 (-5.3 to 1.1)	0.19		
POL6326	41.7 \pm 2.1	45.0 \pm 2.2	3.1 (-0.1 to 6.3)	0.06	5.2 (0.6 to 9.7)	0.027

4, 6, 8, and 10 d after MI, pigs were treated intravenously with POL6326 (n=16) or vehicle-only (control, n=16). 3 d and 6 weeks after MI, infarct volume and left ventricular end-diastolic and end-systolic volumes (LVEDV, LVESV) were determined by contrast-enhanced MRI. LVEF, LV ejection fraction. Changes from 3 d to 6 weeks and treatment effects (POL6326 vs. control) are expressed as differences in least-squares means with 95% confidence intervals (CI) (ANCOVA model with adjustment for 3 d values).



Circulation

Figure Legends

Figure 1. POL5551 mobilizes inflammatory cells and promotes therapeutic effects after

myocardial infarction (MI). (A) Experimental setup for all panels except panel (F). MI was induced in wild-type (WT) mice. Additional mice underwent sham surgery. POL5551 (POL) or vehicle only (control, con) were i.p. injected 2, 4, 6, and 8 d after MI. (B) Neutrophil, monocyte, and lymphocyte numbers in the peripheral blood. 3–5 mice per time point. (C) Ki67⁺ isolectin B4 (IB4)⁺ endothelial cells in the infarct border-zone 3 d after MI. Representative fluorescent images (scale bar, 100 μ m). Summary data from 5 mice per group. * $P < 0.05$ (2-independent-sample t test). (D) CD31⁺ capillary density and IB4⁺ CD31⁺ perfused capillary density in the border-zone 7 d after MI. For quantification, cardiomyocyte (CM) borders were visualized by wheat germ agglutinin (WGA) staining. Scale bar, 100 μ m. Data from 4 control and 5 POL5551-treated mice. ** $P < 0.01$ (2-independent-sample t test). (E) Fluorescein-labeled IB4⁺ capillary density in the border-zone 1, 3, 7, and 28 d after MI. Extracellular matrix and CM borders were highlighted by WGA staining. Fluorescent images were taken at 28 d (scale bar, 50 μ m). Data from 7 sham-operated mice (28 d) and 6–14 infarcted mice per group and time point. * $P < 0.05$, *** $P < 0.001$ vs. sham (for each treatment arm, 1-way ANOVA with Dunnett post hoc test). # $P < 0.05$, ### $P < 0.001$, POL5551 vs. control (2-independent-sample t test). (F) MI was induced in Tie2-GFP mice. After 24 h, tissue samples from the infarcted region were removed and cultured for 3 d in the absence (con) or presence of vascular endothelial growth factor A (VEGFA, 50 ng/mL) or POL5551 (concentration range covering the mean and maximum plasma concentrations after a bolus injection of 8 mg/kg POL5551 in mice).²¹ Images showing GFP fluorescence (scale bar, 500 μ m). Bar graph depicts average sprout length. Explants from 3–6

mice per group. $**P<0.01$ vs. control (1-way ANOVA with Dunnett post hoc test). (G) Scar size 28 d after MI. Tissue sections stained with Masson's trichrome. Data from 12 mice per group. $**P<0.01$ (2-independent-sample t test). (H) and (I) 16 sham-operated mice, 20 infarcted control mice, 21 infarcted POL5551-treated mice. (H) Left ventricular (LV) end-diastolic area (LVEDA) and LV end-systolic area (LVESA) as determined by echocardiography 7 and 28 d after sham surgery or MI. LVEDA and LVESA: $P<0.001$, MI vs. sham for both treatment groups at both time points (1-way ANOVA with Dunnett post hoc test). LVEDA: $P<0.05$, control vs. POL5551-treated mice at 28 d; LVESA: $P<0.01$, control vs. POL5551 at 7 d, $P<0.001$, control vs. POL5551 at 28 d (2-independent-sample t tests). (I) Fractional area change (FAC). Circles represent individual mice. Horizontal bars are the means. $***P<0.001$ vs. both MI groups at each time point (1-way ANOVA with Dunnett post hoc test). $###P<0.001$ (2-independent-sample t tests).

Figure 2. Splenectomy abolishes the therapeutic effects of POL5551. (A) Experimental setup. Myocardial infarction (MI) was induced in wild-type (WT) mice. Additional mice underwent sham surgery. POL5551 (POL) or vehicle only (control, con) were i.p. injected 2, 4, 6, and 8 d after MI. Infarcted mice underwent splenectomy (SPX) immediately before the first injection. (B) Fluorescein-labeled isolectin B4 (IB4)⁺ capillary density in the infarct border-zone 28 d after MI. CM, cardiomyocyte. 6 mice per group. (C) Scar size 28 d after MI. 14 mice per group. (D) and (E) 20 sham-operated mice, 19 control mice, 19 POL5551-treated mice. (D) Left ventricular (LV) end-diastolic area (LVEDA) and LV end-systolic area (LVESA) as determined by echocardiography 28 d after sham surgery or MI. LVEDA and LVESA: $P<0.001$, MI vs. sham

for both treatment groups (2-way ANOVA with Tukey post hoc test). (E) Fractional area change (FAC). *** $P < 0.001$ vs. both MI groups (2-way ANOVA with Tukey post hoc test).

Figure 3. Importance of splenic mononuclear cells for the therapeutic effects of POL5551.

(A) Experimental setup for panels (B) through (E). Sham or myocardial infarction (MI) surgeries were performed in wild-type (WT) donor mice. 2 d after MI, donor mice were i.p. injected with POL5551 (POL) or vehicle only (control, con), and splenic mononuclear cells (MNCs) were isolated 24 h later. Recipient WT mice underwent MI surgery, were splenectomized after 2 d, and then i.v. infused with donor MNCs. (B) through (E) 9–11 mice per group. (B) Fluorescein-labeled isolectin B4 (IB4)⁺ capillary density in the infarct border-zone 28 d after MI. CM, cardiomyocyte. (C) Scar size 28 d after MI. (D) Left ventricular (LV) end-diastolic area (LVEDA) and LV end-systolic area (LVESA) as determined by echocardiography 28 d after MI. LVESA: $P < 0.05$, recipients receiving MNCs from infarcted POL5551-treated vs. infarcted vehicle only-treated donors (2-independent-sample t test). (E) Fractional area change (FAC). (F) Experimental setup for panels (G) and (H). MI was induced in WT donor and recipient mice. 2 d after MI, donor mice were i.p. injected with POL5551 or vehicle only (con) and splenic monocytes were isolated 24 h later. 2 d after MI, recipient mice were splenectomized and then i.v. infused with donor monocytes. 7–8 mice per group. (G) LVEDA and LVESA 28 d after MI. (H) FAC. ** $P < 0.01$, *** $P < 0.001$ (2-independent-sample t tests).

Figure 4. Importance of regulatory T cells for the therapeutic effects of POL5551.

(A) Experimental setup. Myocardial infarction (MI) was induced in DERE mice. Diphtheria toxin (DT) or saline were i.p. injected immediately before and 24 h after MI. POL5551 (POL) or

vehicle only (control, con) were i.p. injected 2, 4, 6, and 8 d after MI. (B) Representative flow cytometry panels confirming $CD4^+ Foxp3^+/eGFP^+$ regulatory T cell depletion in splenocytes 24 h after the second DT injection. (C) through (F) 8–9 mice per group. (C) Fluorescein-labeled isolectin B4 (IB4)⁺ capillary density in the infarct border-zone 28 d after MI. CM, cardiomyocyte. (D) Scar size 28 d after MI. (E) LV end-diastolic area (LVEDA) and LV end-systolic area (LVESA) as determined by echocardiography 28 d after MI. LVESA: $P < 0.05$, POL5551 vs. control in saline-injected mice (2-independent-sample t test). (F) Fractional area change (FAC). * $P < 0.05$, ** $P < 0.01$, *** $P < 0.001$ (2-independent-sample t tests).

Figure 5. Splenic regulatory T cells are required and sufficient for the therapeutic effects of

POL5551. (A) Experimental setup for panels (B) through (E). Myocardial infarction (MI) was induced in DEREK donor and wild-type (WT) recipient mice. Donor mice were i.p. injected with diphtheria toxin (DT) or saline immediately before and 24 h after MI. 2 d after MI, donor mice were i.p. injected with POL5551 (POL), and splenic mononuclear cells (MNCs) were isolated 24 h later. 2 d after MI, recipient mice were splenectomized and then i.v. infused with donor MNCs. (B) through (E) 5 mice treated with MNCs from saline-injected donors, 6 mice treated with MNCs from DT-injected donors. (B) Fluorescein-labeled isolectin B4 (IB4)⁺ capillary density in the infarct border-zone 28 d after MI. CM, cardiomyocyte. (C) Scar size 28 d after MI. (D) Left ventricular (LV) end-diastolic area (LVEDA) and LV end-systolic area (LVESA) as determined by echocardiography 28 d after MI. (E) Fractional area change (FAC). (F) Experimental setup for panels (H) through (K). MI was induced in DEREK donor and WT recipient mice. 2 d after MI, donor mice were i.p. injected with POL5551 or vehicle only (control, con) and splenic $CD4^+ Foxp3^+/eGFP^+$ regulatory T (T_{reg}) cells were isolated 24 h later.

2 d after MI, recipient mice were splenectomized and then i.v. infused with donor T_{reg} cells.

(G) Representative flow cytometry panels showing unsorted splenic MNCs (left) and sorted splenic T_{reg} cells (right) that were used for transplantation. CD4⁺ Foxp3⁺/eGFP⁺ T_{reg} cells are highlighted in both panels. (H) through (K) 6 mice that received T_{reg} cells from vehicle only-treated donors, 6 mice that received T_{reg} cells from POL5551-treated donors. (H) Capillary density in the border-zone 28 d after MI. (I) Scar size 28 d after MI. (J) LVEDA and LVESA 28 d after MI. (K) FAC. (L) Experimental setup for panels (N) through (Q). MI was induced in CD11c-Cre iDTR donor and WT recipient mice. Donor mice were i.p. injected with DT or saline 24 h and immediately before MI. 2 d after MI, donor mice were i.p. injected with POL5551, and splenic MNCs were isolated 24 h later. 2 d after MI, recipient mice were splenectomized and then i.v. infused with donor MNCs. (M) Representative flow cytometry panels showing non-dendritic cell (DC)-depleted (saline) and DC-depleted (DT) splenic MNCs that were used for transplantation. DCs are highlighted in all panels. (N) through (Q) 7 mice treated with MNCs from saline-injected donors, 6 mice treated with MNCs from DT-injected donors. (N) Capillary density in the border-zone 28 d after MI. (O) Scar size 28 d after MI. (P) LVEDA and LVESA 28 d after MI. LVESA: P<0.05 (2-independent-sample t test). (Q) FAC. *P<0.05, **P<0.01 (2-independent-sample t tests).

Figure 6. POL5551 enhances regulatory T cell mobilization, cardiac recruitment, and immune-modulatory function. (A) and (B) Myocardial infarction (MI) was induced in DERE mice and POL5551 (POL) or vehicle only (control, con) were i.p. injected after 2, 4, 6, and 8 d. CD4⁺ Foxp3⁺/eGFP⁺ regulatory T (T_{reg}) cell numbers (A) in the peripheral blood and (B) in the infarcted left ventricle (LV). 3–9 mice per time point. (C) CD4⁺ Foxp3⁺/eGFP⁺ T_{reg} cell numbers

in the infarcted and noninfarcted (remote) region 2 h after the 1st vehicle only (con) or POL5551 injection. 5 mice per group. (D) and (E) 2 d after MI, DERE mice underwent splenectomy or sham surgery (laparotomy only, LAP) and were then i.p. injected with POL5551 or vehicle only (con). CD4⁺ Foxp3⁺/eGFP⁺ T_{reg} cell numbers (D) in the peripheral blood 2 h later and (E) in the infarcted LV 24 h later. 4–9 mice per group. (F) MI was induced in DERE donor and wild-type recipient mice. 2 d after MI, donor mice were injected with POL5551 or vehicle only (con) and splenic mononuclear cells (MNCs) were isolated 24 h later. 2 d after MI, recipient mice were splenectomized and then i.v. infused with 17×10^6 donor MNCs (as shown in a pilot experiment, MNCs from POL5551- and vehicle only-treated donors contained comparable numbers of CD4⁺ Foxp3⁺/eGFP⁺ T_{reg} cells). 2 h later, T_{reg} cells were quantified in the infarcted region in recipient mice. 11 mice per group. (G) DERE mice were i.p. injected with diphtheria toxin (DT) or saline immediately before and 24 h after MI. 2 d after MI, mice were i.p. injected with POL5551 or vehicle only (con). 2 d later, Ly6C^{low/high} monocytes and macrophages were isolated from the infarcted region and the expression levels of tumor necrosis factor (TNF), interleukin 1 β (IL-1 β), interferon γ (IFN- γ), nitric oxide synthase 2 (NOS2), interleukin 10 (IL-10), and transforming growth factor β 1 (TGF- β 1) were determined by RT-qPCR. 8–10 mice per group. *P<0.05, **P<0.01, ***P<0.001 (2-independent-sample t tests).

Figure 7. Continuous POL5551 infusion mobilizes regulatory T cells but prevents their cardiac recruitment and therapeutic effects. (A) Expression levels of C-X-C motif chemokine ligand 12 (CXCL12) in the infarcted region at various time points after myocardial infarction (MI) or sham operation (d 7) as determined by RT-qPCR. 5–9 mice per group. **P<0.01, ***P<0.001 vs. sham (1-way ANOVA with Dunnett post hoc test). (B) Experimental setup for

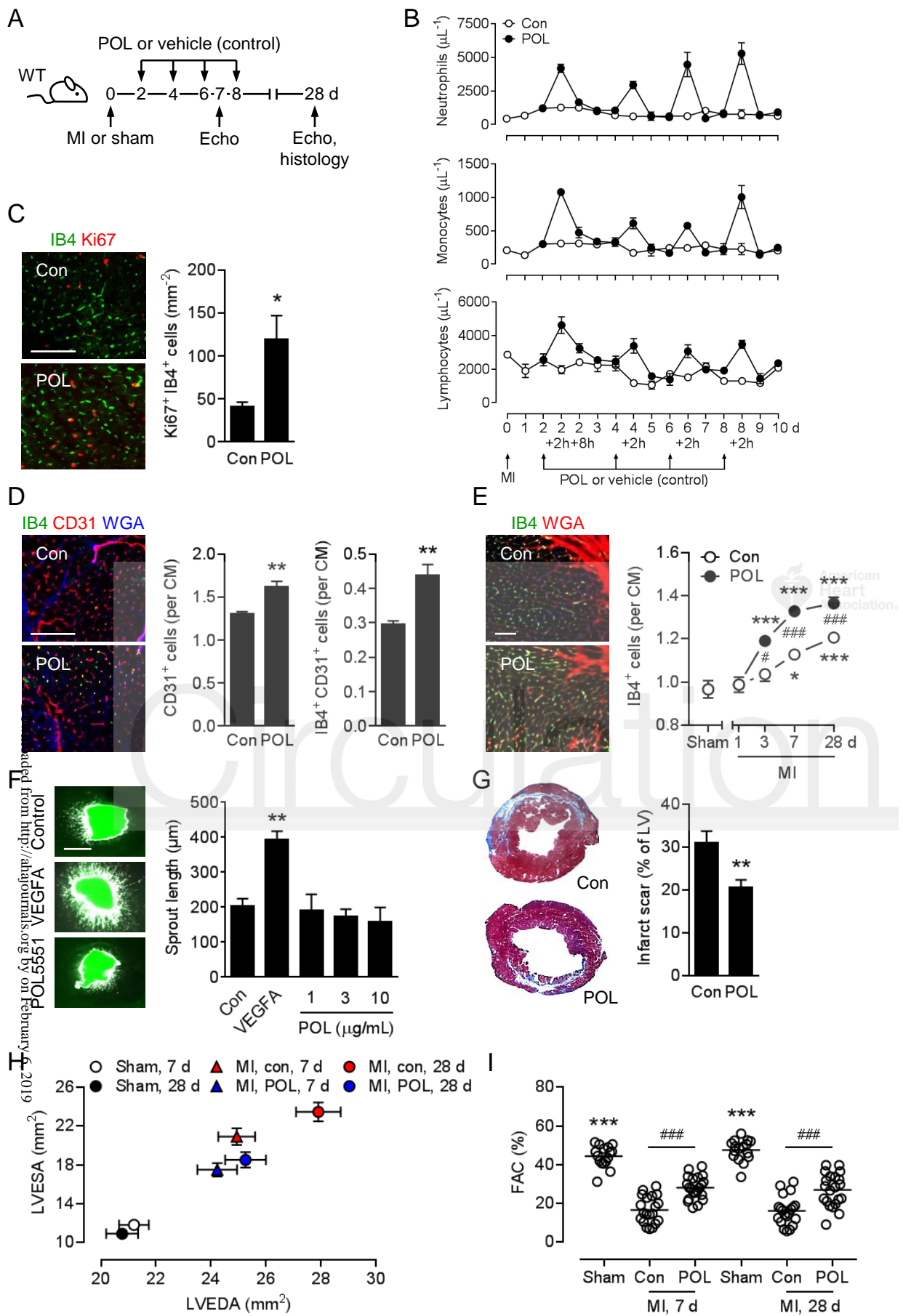
panels (C) and (D). MI was induced in DERE mice. POL5551 (POL) or vehicle only (control, con) were i.p. injected 2 and 4 d after MI or s.c. infused starting 2 d after MI.

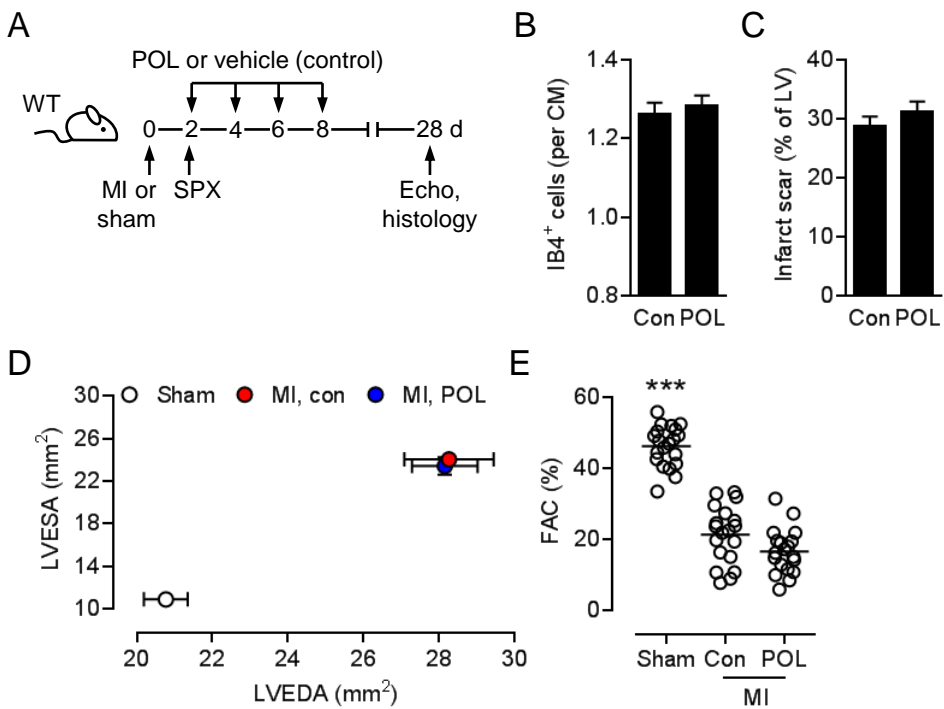
(C) CD4⁺ Foxp3⁺/eGFP⁺ regulatory T (T_{reg}) cell numbers in the peripheral blood and (D) in the infarcted region at 4 d + 2 h after MI. 4–5 mice per group. (E) Experimental setup for panels (F) through (I). MI was induced in wild-type (WT) mice. POL5551 or vehicle only (con) were i.p. injected 2, 4, 6, and 8 d after MI or s.c. infused for 7 d starting 2 d after MI. 5–7 mice per group.

(F) Fluorescein-labeled isolectin B4 (IB4)⁺ capillary density in the infarct border-zone 28 d after MI. CM, cardiomyocyte. (G) Scar size 28 d after MI. (H) Left ventricular (LV) end-diastolic area (LVEDA) and LV end-systolic area (LVESA) as determined by echocardiography 28 d after MI. LVEDA: P<0.05, POL5551 vs. vehicle only boluses; LVESA: P<0.001, POL5551 vs. vehicle only boluses (2-independent-sample t tests). (I) Fractional area change (FAC). *P<0.05

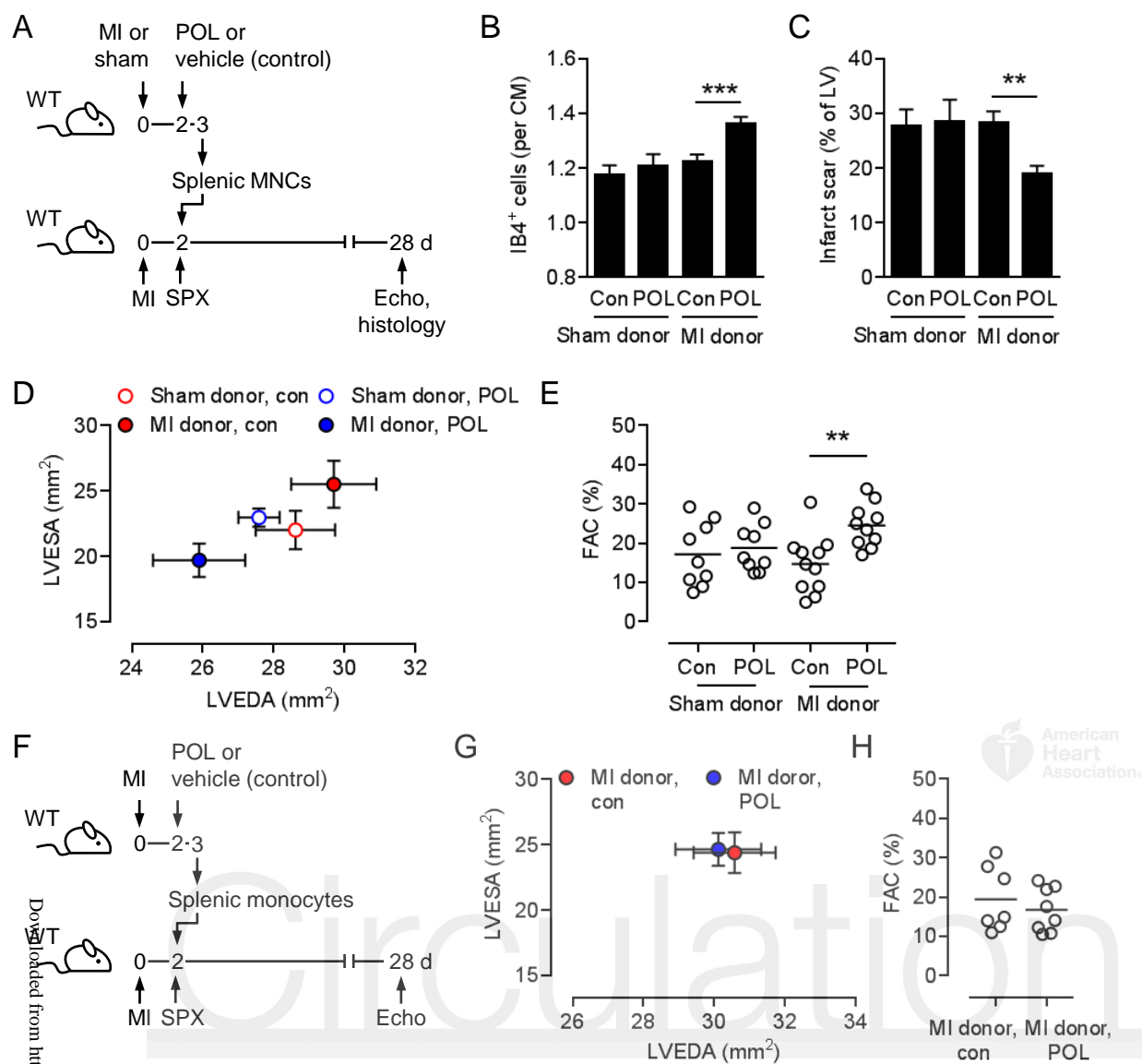
(2-independent-sample t tests).

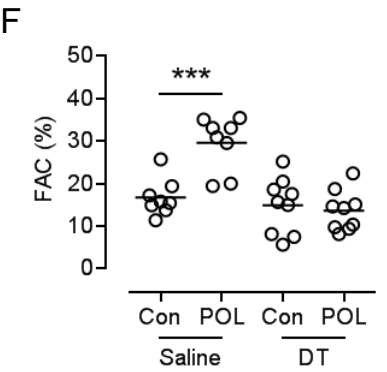
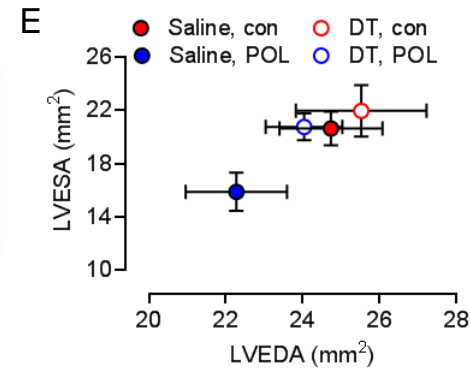
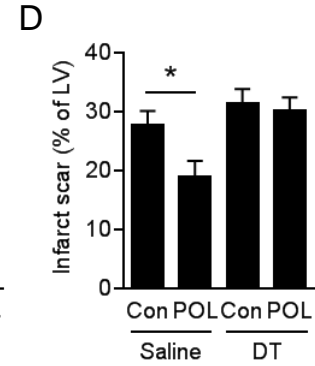
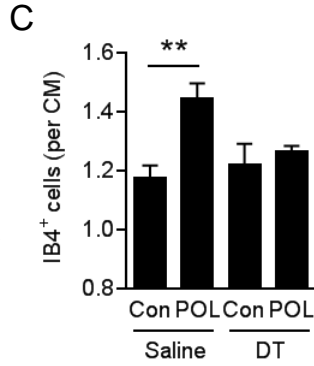
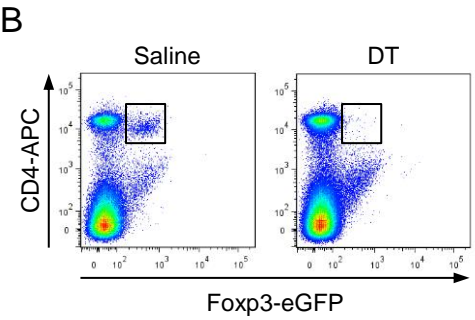
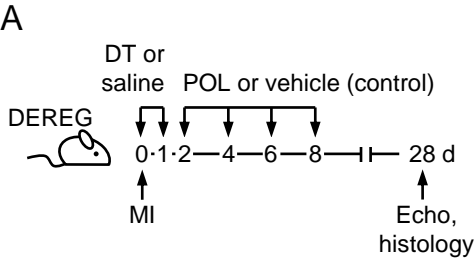
Circulation





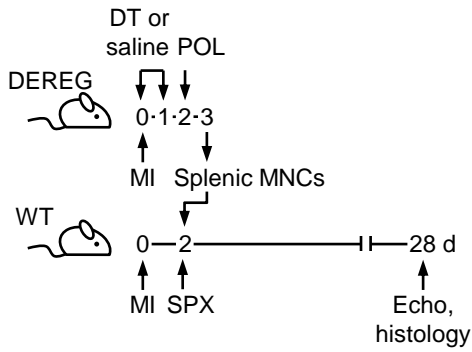
Circulation



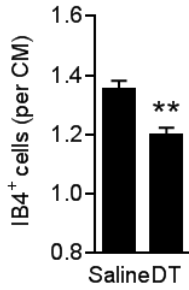


Circulation

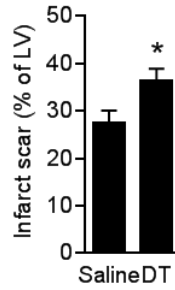
A



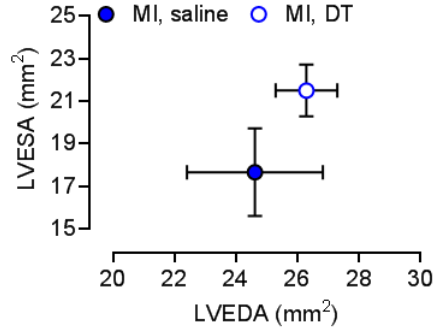
B



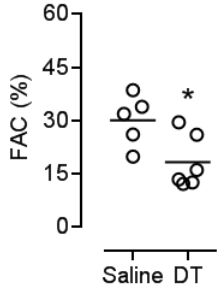
C



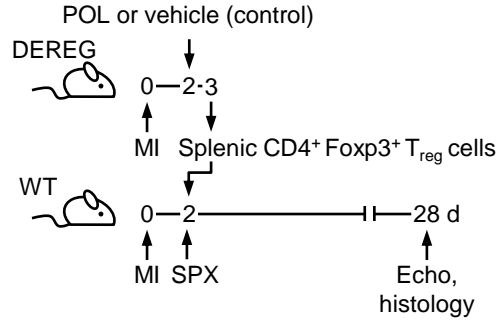
D



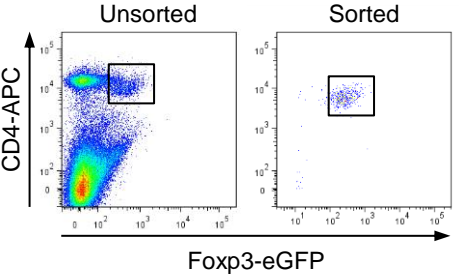
E



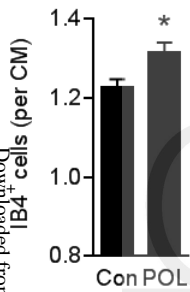
F



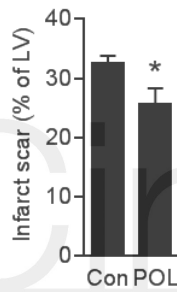
G



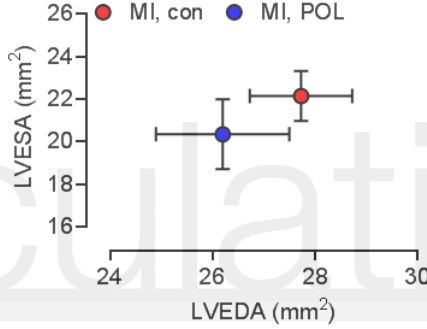
H



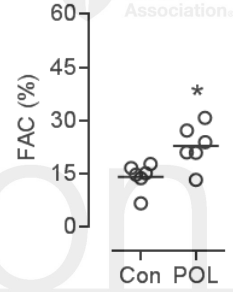
I



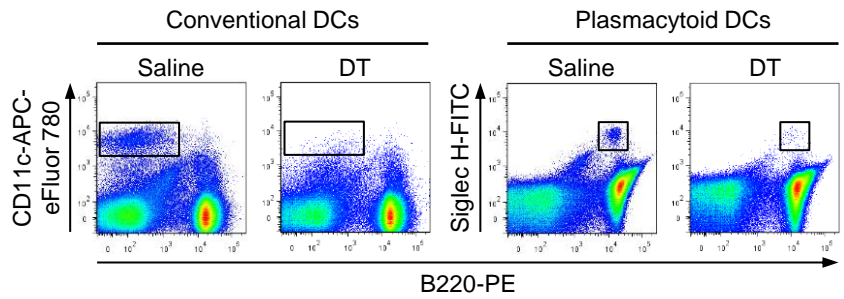
J



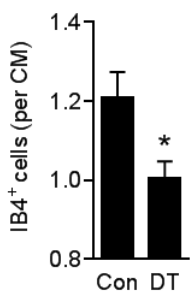
K



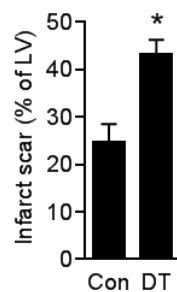
M



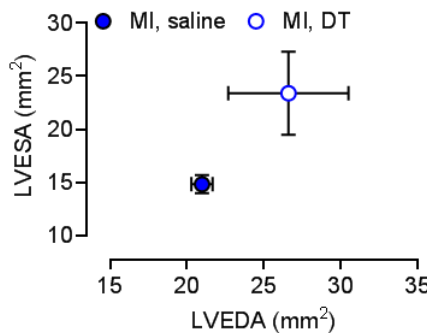
N



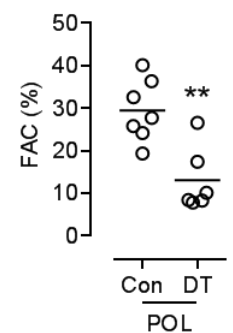
O

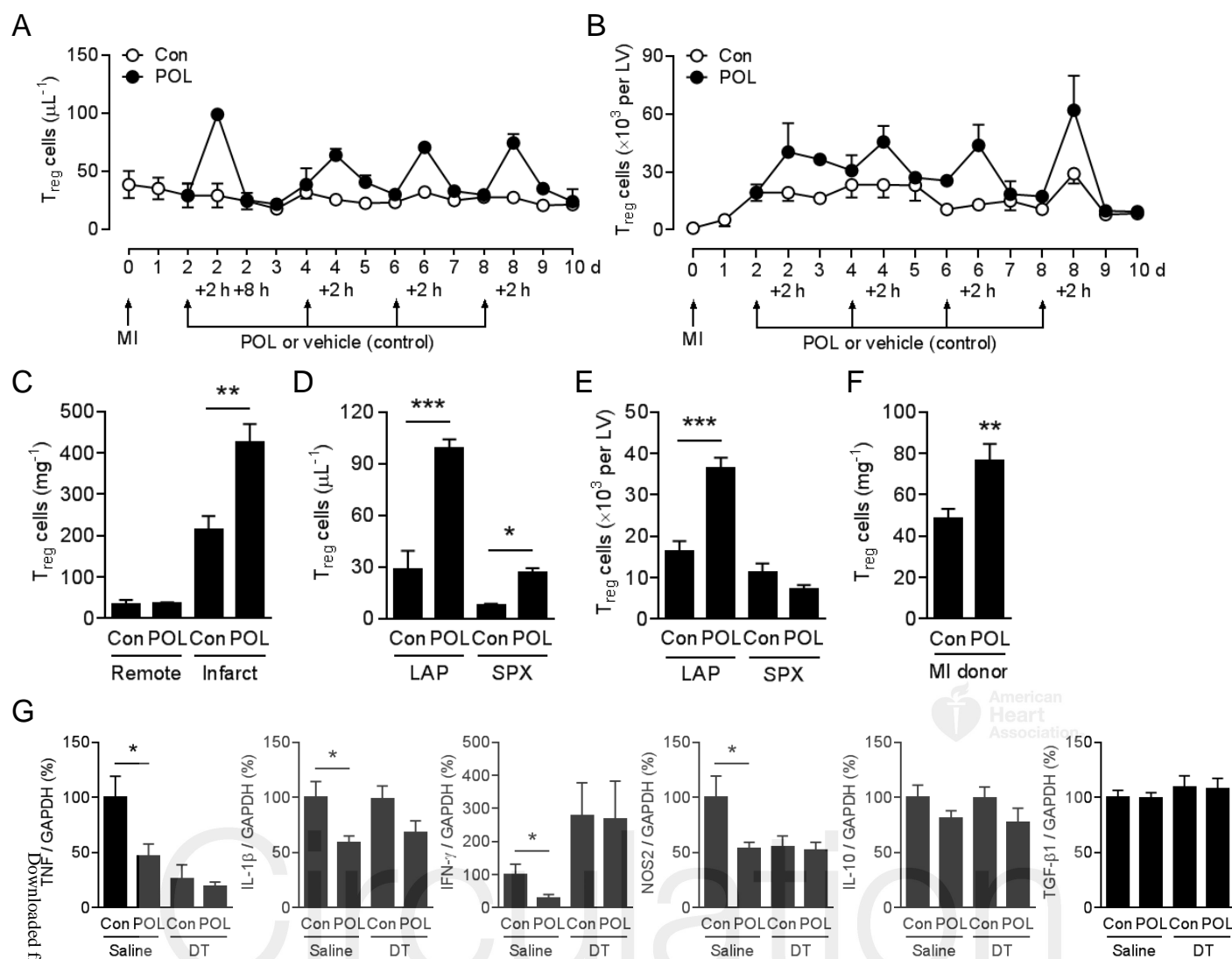


P

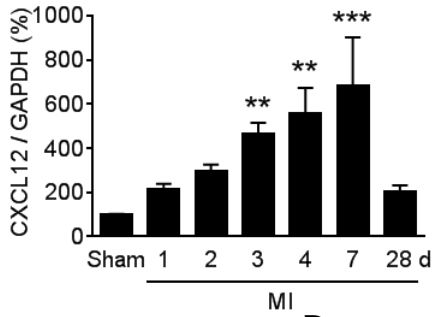


Q

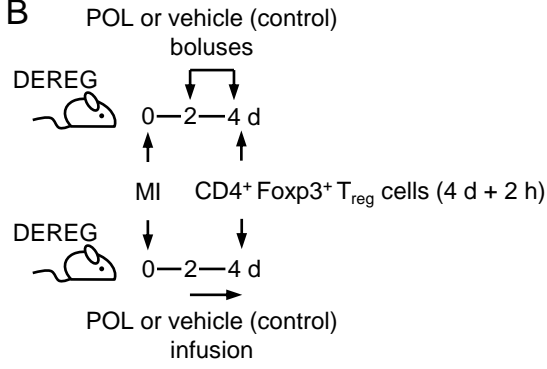




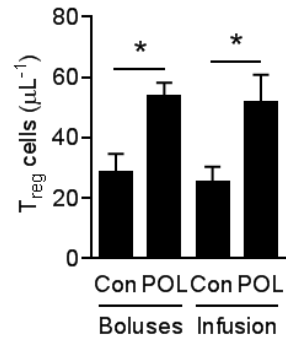
A



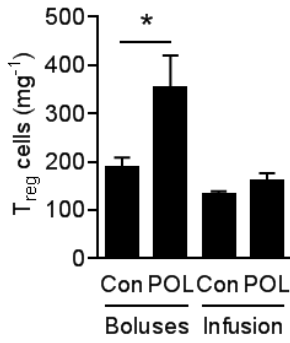
B



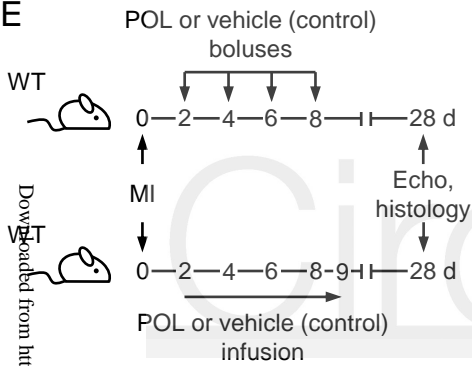
C



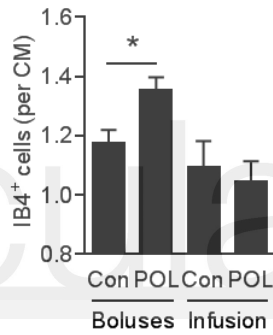
D



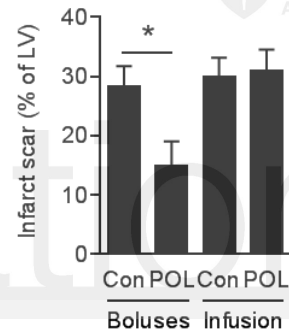
E



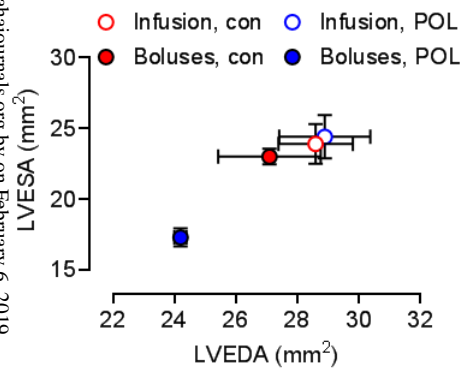
F



G



H



I

